Journal of Instrumentation

PAPER • **OPEN ACCESS**

The high voltage system the novel MPGD-based photon detectors of COMPASS RICH-1 and its development towards a scalable HVPSS for MPGDs

To cite this article: A. Bressan *et al* 2023 *JINST* **18** C07014

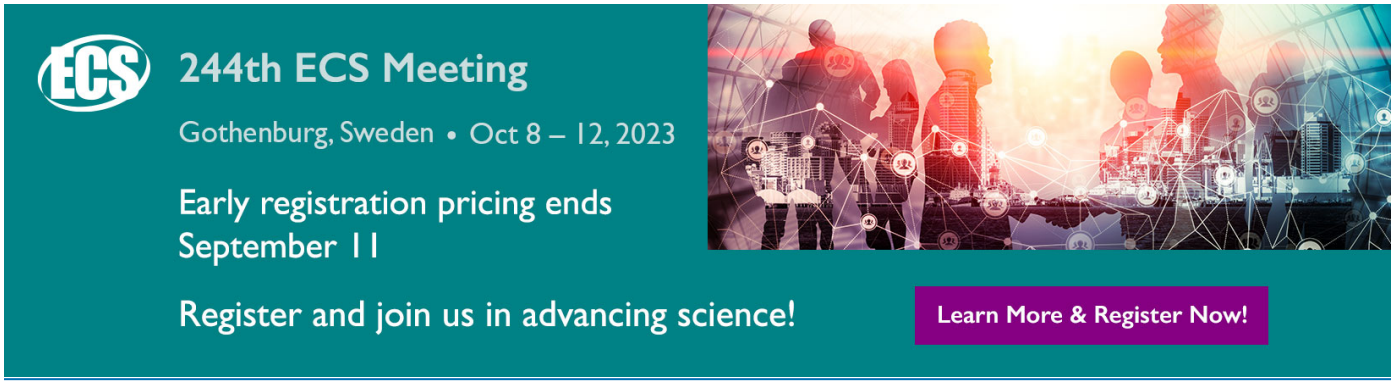

Published by IOP Publishing for Sissa Medialab
Received: *March 27, 2023*
Accepted: *June 5, 2023*
Published: *July 18, 2023*
7TH International Conference on Micro Pattern Gaseous Detectors
Rehovot, Israel
11–16 December 2022

The high voltage system the novel MPGD-based photon detectors of COMPASS RICH-1 and its development towards a scalable HVPSS for MPGDs

A. Bressan,[a,b] **S. Carrato,**[b] **C. Chatterjee,**[a] **A. Cicuttin,**[c,a] **M.L. Crespo,**[c,a] **D. D'Ago,**[a,b] **S. Dalla Torre,**[a] **S. Dasgupta,**[a,1] **M.G. Ballina Escobar,**[c] **W.F. Samayoa,**[c,b,a] **L. García Ordóñez,**[c,b,a] **M. Gregori,**[a] **G. Hamar,**[a,2] **A. Kosoveu,**[a] **S. Levorato,**[a,d,*] **K. Mannatunga,**[c] **A. Martin,**[a,b] **F. Tessarotto,**[a] **Triloki**[a,c] **and B. Valinoti**[c,b,a]

[a] *INFN, Sezione di Trieste, Trieste, Italy*
[b] *Trieste University, Trieste, Italy*
[c] *ICTP, Trieste, Italy*
[d] *European Organization for Nuclear Research, Geneva, Switzerland*

E-mail: stefano.levorato@cern.ch

Abstract: The COMPASS RICH-1 detector underwent major upgrade in 2016 with the installation of four novel MPGD-based photon detectors. They consist of large-size hybrid MPGDs with multi-layer architecture composed of two layers of Thick-GEMs and bulk resistive Micromegas. A dedicated high voltage power supply system, realized with commercial devices, has been put in operation to protect the detectors against errors by the operator, monitor and log voltages and currents at a 1 Hz rate, and automatically react to detector misbehavior; it includes also the HV compensation for the detector gas pressure and temperature variations.

The needs posed to the high voltage power supply systems by the operation of Micro Pattern Gaseous Detectors pushed the development of a novel single channel HV system able to overcome the performance of the commercial devices in terms of high-resolution diagnostic features and intelligent dynamic voltage control. In this talk the COMPASS HV system and its performance are illustrated, as well as the stability of the novel MPGD-based photon detectors during the physics data taking at COMPASS. The performance of the novel single channel power supply system when connected to a single photon Micro Pattern Gaseous Detector is presented in realistic working condition during a test beam with the preliminary results of multiple channels operation.

Keywords: Cherenkov detectors; Micropattern gaseous detectors (MSGC, GEM, THGEM, RETHGEM, MHSP, MICROPIC, MICROMEGAS, InGrid, etc); Photon detectors for UV, visible and IR photons (gas)

[1] Now at National Institute of Science Education and Research, Bhubaneswar, India.
[2] Now at Wigner Research Centre for Physics Hungarian Academy of Sciences Budapest, Hungary.
[*] Corresponding author.

https://doi.org/10.1088/1748-0221/18/07/C07014

Contents

2023 JINST 18 C07014

1 Architecture of the COMPASS RICH-1 Gaseous Micro Pattern Photon Detectors

During the 2015–2016 winter shut-down of the COMPASS [1] experiment, approximately 1.4 m^2 of the active area of the RICH-1 [2–4] Photon Detectors (PD) was upgraded by novel detectors based on Micro Pattern Gaseous Detector technologies with unit size of $600 \times 600\,mm^2$.

The architecture of the novel detectors, illustrated in figure 1a, combines in a hybrid MPGD arrangement two layers of THick GEMs [5] (THGEM) to a MicroMegas [6] (MM). The top surface of the first THGEM is coated with a CsI film which acts as a reflective photo-cathode. THGEMs are 0.4 mm thick, hole diameter and pitch are 0.4 mm and 0.8 mm respectively. The MM uses a pad segmented anode with a pad size of $7.5 \times 7.5\,mm^2$ and 8 mm pitch. Each hybrid detector is made by two $600 \times 300\,mm^2$ modules placed side by side to form a single unit: see figure 1b, c. The bulk MM adopts an original implementation making use of discrete resistive elements: HV is

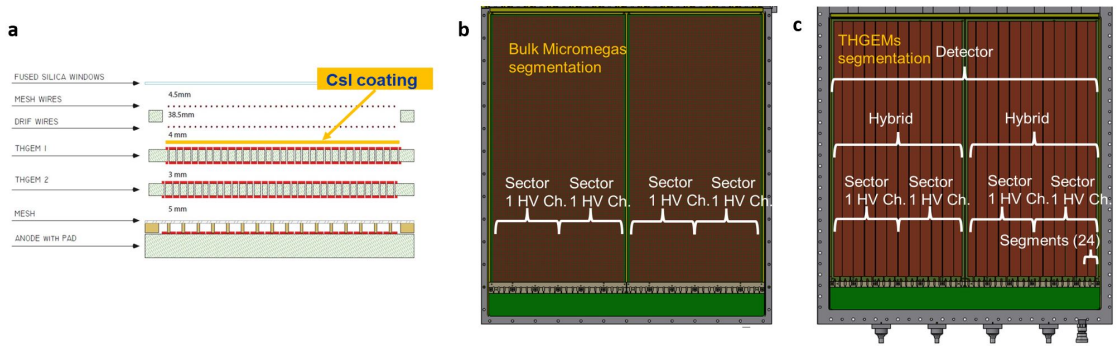

Figure 1. a: sketch of the hybrid single photon detector: two staggered THGEM layers are coupled to a bulk MM. The drift wire and protection plane are visible. b) Segmentation of the MM detector. c) Segmentation of the THGEM layers. Image not to scale.

applied to the anode pads, each one protected by an individual 470 MΩ resistor, while the signals are collected from a second set of pads, parallel to the first ones, embedded in the anode PCB, where the signal is transferred by capacitive coupling. The large-value resistance decouples each pads from the neighboring ones in case of occasional discharges limiting the voltage (gain) drop to 2 V (4%) [7]. The pads HV is distributed via 4 independent HV Channels to the corresponding MM

sectors (figure 1b) and figure 2a) and b). Both surfaces of each THGEM [9] unit ($600 \times 300\,\mathrm{mm}^2$) are divided into 12 electrodes, referred as segments. The segments of the top and bottom THGEM face are grouped by six forming two sectors per THGEM unit, namely four per THGEM plane in a detector (figure 1c). A sector is powered via an independent single HV channel through a distribution scheme employing a 1 GΩ resistors and fast 20ETS12S[1] diodes to prevent the current flow from a segment to the others in case of a discharge as shown in figure 2c).

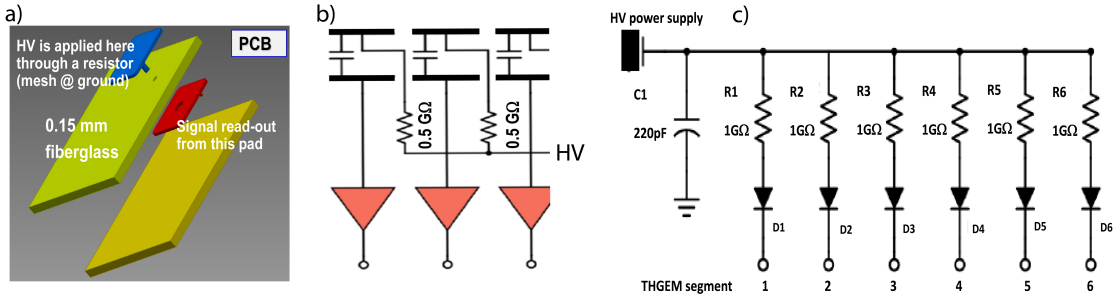

Figure 2. a) Sketch of the PCB layers illustrating the principle of readout design. The blue (external) pad is the anode electrode of the MM, the red (internal) pad is embedded in the PCB and the signal is transferred from the blue to the red pad by capacitive coupling. b) The principle is illustrated by the electrical scheme. The top elements of the capacitors are the pad forming the MM anode (blue (external) pad in a)), the bottom elements of the capacitors (red (internal) pad in a)) are connected to the front-end electronics. c) Scheme of the voltage distribution of the top (bottom) face of a THGEM sector containing 6 segments.

The detectors are operated with the gas mixture Ar : CH4 = 50 : 50, selected for optimal extraction of the photo-electrons from the converting CsI film to the gaseous atmosphere. The typical voltages applied to the detector electrodes are 1270 V across THGEM1, 1250 V across THGEM2, and 620 V to bias the MM. The drift field above the first THGEM is 500 V/cm, the transfer field between the two THGEMs is 1000 V/cm and the field between the second THGEM and the MM micromesh is 1000 V/cm. This corresponds to effective gain-values for the three multiplication layers around 12, 10 and 120 for a total effective gain of ≈15k.

2 The HV system and its control software

The HV system requirements are dictated by the need of current monitoring with fine resolution to control MPGD operation and by the multistage architecture of the novel detectors with strongly correlated applied voltages. Electrode segmentation results in further complexity of the control of the system. The High Voltage Control System (HVCS) implements automatic protocols, for ≈ 140 HV channels, to react to occasional misbehavior of the detectors and to adapt the supply voltages to the environmental changes in pressure (P) and temperature (T) to maintain the detector gain constant.

Two different power supply units by CAEN[2] have been selected: THGEM electrodes as well as the protection wires and the drift wires are powered by A1561HDN 12-channel fully floating power modules, characterized by a low voltage ripple, typically 5 mV pp from 10 Hz to 100 MHz at full load, fine voltage resolution, 100 mV for setting and 10 mV for monitoring, and the fine current resolution, 500 pA for setting the maximum current and 50 pA for monitoring. These figures

[1] VS-20ETS12S-M3 Series — Vishay.
[2] CAEN https://www.caen.it/.

2023 JINST 18 C07014

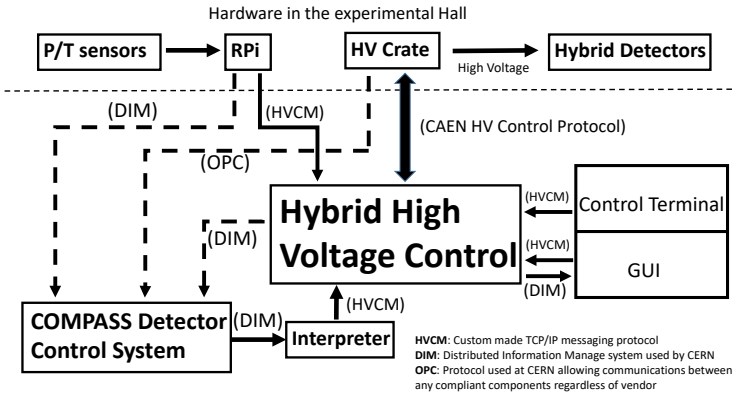

Figure 3. Block diagram of the hybrid high voltage control system, showing the components and their communication channels.

have been confirmed in operation. MM pads are supplied by A7030DP 12-channel fully floating modules. The choice of fully floating HV units allows for a very convenient on-detector ground reference, namely the detector frames. With the implemented scheme approximately 25 independent HV channels are needed for the biasing of each detector.

The temperature and pressure measurement is performed via the ADT7420[3] sensor, with ±0.25 °C accuracy, and the MS5611-01BA03[4] barometric pressure sensor with an accuracy of ±2.5 hPa. Eight couples of sensors are read, one at the entrance one at the exit of the gas lines of each detector: the sensors are mounted on a dedicated narrow PCB (100 mm × 7.5 mm), together with an IP674-pin M8 connector to allow sensors readout. The PCB mechanical support allows direct mounting on the chambers' frames inside the detector volume in contact with the gas. The sensor boards are connected to the readout board via 4-cores cables which are up to 7 m-long. The output is connected to Raspberry Pi 3 Model B SBC [8] via its GPIO interface. The gas P and T parameters are sent, via the experiment internal network to the High Voltage Control System PC (HVCS-PC) for logging and voltage adjustment according to the block scheme illustrated in figure 3. For a detailed description of the communication system between the Raspberry Pi and the HVCS-PC, the voltage adjustment protocol and the detailed description of the integration with the Detector Control System (DCS) of the experiment the reader is refereed to the following [9]. For the THGEM with the geometric parameters employed for the RICH-1 PD an increase of 1 V will result in a 1% gain increase, while for MM it will result in a 2% gain increase for the gas mixture employed. A temperature variation of 5 K requires a voltage compensation of about ≈1% for each multiplication stage, while it would cause a gain variation of ≈40% if not compensated. Similarly, a variation of 10 mbar can be compensated by a $\Delta V = 0.5\%$, while it would cause a gain variation of ≈20% if not compensated [9]. An excellent gain uniformity has been reached over the segments of the detectors by the fine adjustment of the single amplification stages: a single sector shows a standard deviation of approximately 5.5%, an excellent result despite the limitations related to the temperature non uniformity of the gas in the detector and the approximations of the gain compensation corrections.

Detector discharges, measured as current peaks by the High Voltage Control System (HVCS) can be correlated among the different multiplication stages: sparks in the two THGEM layers of a

[3]ADT7420 — Analog Devices.
[4]The MS5611-01BA03 — MEAS.

2023 JINST 18 C07014

sector are 100% correlated. The spark rate in MM is low compared to THGEMs, a MM discharge is accompanied by a spark in THGEMs in 70% of the cases. MM discharges have a duration of 1–2 s, while THGEM ones last 10 s. These short duration combined with the very low discharge rate of the order of 1/h per detector as well as its segmentation, which limits the area affected by a spark, makes the dead-time caused by detector sparks totally negligible [9]. The HVCS connects to the slow control system of the experiment DCS system and offers the experts control and log of the full detector data via the Distributed Information Management (DIM) servers at 1 Hz rate.

3 The High Voltage Power Supply System for MPGD

The development of a High Voltage Power Supply System (HVPSS) [10] suited for the MPGD technologies originates from the experience gained in upgrading COMPASS RICH-1 with MPGD-based single photon detectors. In particular it allows to perform MPGD R&D when the monitoring of the voltage and current parameters in a time windows of the order of few ns is needed. The system has been designed and built initially as a single HV channel unit but with scalability properties in view of the realization of a multichannel system. The HVPSS driving motivation is the matching of all the requirements for the complete monitoring and the accurate HV handling of MPGDs that cannot be satisfied using commercial power supply systems; in particular when the monitoring of the voltage and current parameters has to be performed with a time resolution in the order of few ns. It has been realized employing the FPGA technology to exploit the possibility to prevent and limit discharge events: this option requires the use of high-speed electronics with re-configurable capabilities able to take decisions using both the information broadcast from neighboring independent channels and environmental variables changes.

The general scheme illustrating the connectivity of the different units of the HVPSS is illustrated in figure 4. The HVPSS is composed of a commercial DC / DC converter based on the ISEG[5] BPn4010512 module capable to deliver up to 4 kV. The voltage control of the DC-to-DC converter is obtained via a 16-bit DAC MAX5216[6] and galvanically isolated through a high-performance quad-channel digital isolator ISO7841DWW[7] with 8 kV peak isolation voltage. A custom made picoammeter board (pA) is built around a AD549LHZ[8] operational amplifier operated in trans-conductance mode. A dedicated data acquisition board for high speed Analog to Digital Conversion (ADC) has been built employing the low power 8-bit high speed 500 MSPS ADC08500 device. The current resolution of the picoammeter coupled with this ADC spans from 3.9 pA at 0.95 MHz to 65.2 pA at 250 MHz, within a full range of 60 nA.

The CIAA-ACC, an open hardware industrial System-on-Chip (SoC) carrier designed by the Argentinian International Institute of Industrial Technology, has been selected for data acquisition and system operation handling. It houses a Xilinx Zynq 7030 FPGA and microprocessor SoC in a high pin count (HPC) FMC carrier compliant with the ANSI VITA 57.1 standard. Logic cores designed and implemented in the FPGA subsystem handle the data acquisition and time-deterministic tasks such as raw data sampling, time-stamping, signal analysis and diagnostics, hardware peripheral

[5]ISEG https://iseg-hv.com/.
[6]MAX5216 https://www.maximintegrated.com/.
[7]ISO7841DWW https://www.ti.com/.
[8]AD549LHZ — ANALOG DEVICES.

2023 JINST 18 C07014

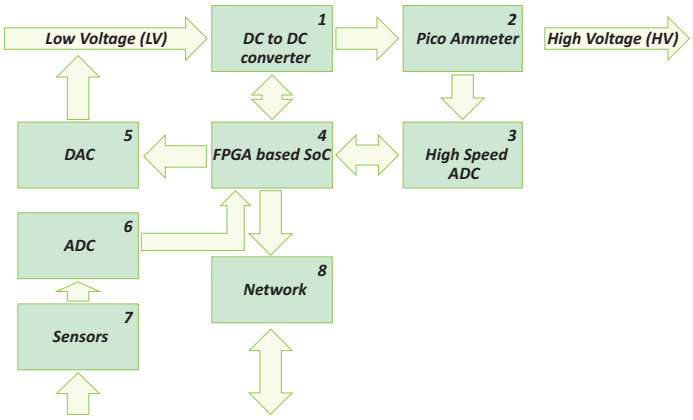

Figure 4. General block diagram of the control system for a single unit high voltage power supply. The HVPSS sub systems are shown and the inter-connectivity of the different elements is indicated by the arrows.

control, and the communication between the FPGA and microprocessor [11]. The microprocessor subsystem handles the slow control and communication with an external PC for each channel. The reading of the pressure and temperature sensors enables the calculation of the corresponding HV compensation by the microprocessors by the following equation $\frac{\Delta V}{\Delta V_0} = 1 + 0.55(\frac{P}{T}\frac{T_0}{P_0} - 1)$. The coefficients of the formula are obtained from the fit of experimental data points of an identical detector operated at various pressure and temperature conditions in laboratory exercises [7] exploiting the Townsend coefficient dependence on the gas density [12].

4 The High Voltage Power Supply System performance

A fully single channel system has been employed during a test beam exercise in October 2018 at CERN SPS H4 beam line [9]. The system has been operated for nearly two weeks powering the MM mesh of the last multiplication stage of a hybrid prototype for single photon detection, recording the current provided to the micro-mesh at the sampling rate of 156 Hz and successfully saving several discharge events at the maximum speed of 500 MHz i.e. 2 ns time resolution. The waveform data were sent and saved to the remote connected PC for offline analysis [10]. After the successful operation of the single channel system a three channels HVPSS module has been operated connected to independent segments of the first THGEM layer of a hybrid photon detector. The time synchronization between the modules has been obtained via Precision Time Protocol (PTP) through a high voltage isolation buffer network interface [13]. The detector electrodes of the prototype have been biased 10% more than the typical operating voltage resulting in a large rate of discharges between the top and bottom layer of the THGEM. A comparison of the current spikes as a function of the detection time taken during several minutes is plotted for the three different channels in figure 5. The red line corresponds to fully correlated events. The diagonal shows a kernel density estimation plot of the time distribution of the electrical discharges on each channel. By choosing an electrical discharge as primal and measuring the elapsed time for the next one in a one-second window, a peak around 600 to 700 milliseconds can be seen in figure 6. As shown in the plot, one of the three channels presents a higher contribution to these events. The results illustrated are obtained in an abnormal working condition of the detector and are shown only to illustrate the system's capabilities.

2023 JINST 18 C07014

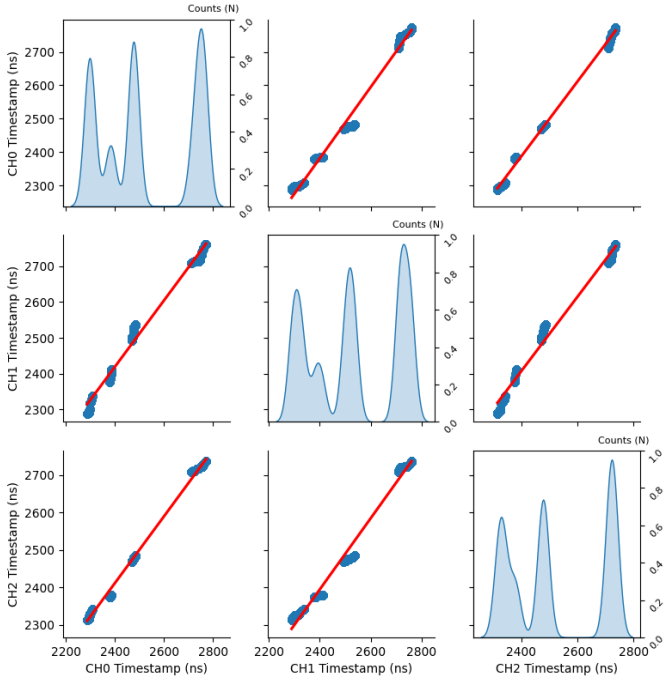

Figure 5. Pairwise scatter plot matrix of discharge times of three neighboring HV channels.

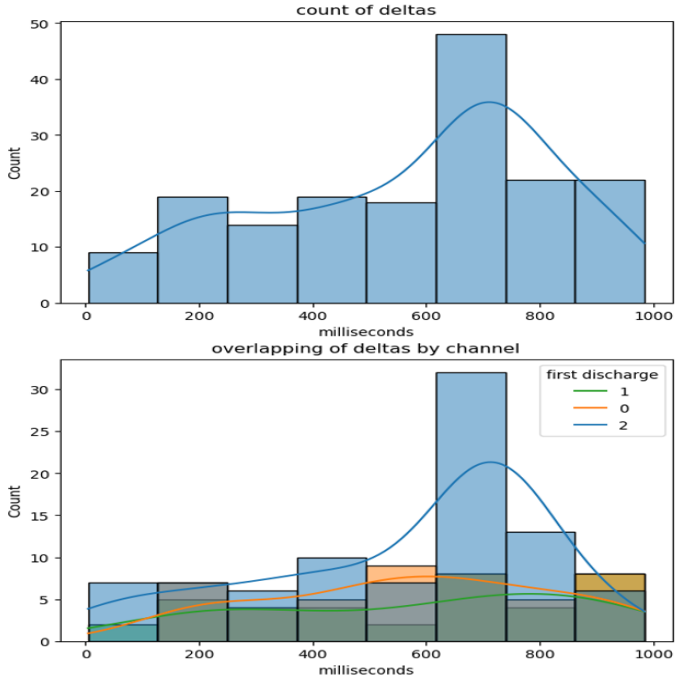

Figure 6. Histogram of time difference (deltas) after primal discharge in a one-second window and the contribution of each channel into the discharges.

2023 JINST 18 C07014

5 Conclusions

Systematic tests are ongoing at the time this article has been written, improving the 20 ns maximum time uncertainty measured between the different HVPSS system synchronization systems via the PTP protocol. The preliminary tests performed with a multi channel system have proven the possibility to operate the HVPSS connected to a single photon MPGD based detector and to record the discharges affecting the detector electrodes with ≈20 ns time resolution: this would have been not possible with a commercial system. The noise figures in terms of HV ripple measured for the CAEN commercial HV power supply and the HVPSS are comparable.

Further tests are needed to confirm the results, to optimize the parameters, to check the long term operation as well as the behavior when all electrodes are connected to larger-size photon detectors.

References

[1] COMPASS collaboration, *The COMPASS experiment at CERN*, *Nucl. Instrum. Meth. A* **577** (2007) 455 [hep-ex/0703049].

[2] E. Albrecht et al., *Status and characterisation of COMPASS RICH-1*, *Nucl. Instrum. Meth. A* **553** (2005) 215.

[3] P. Abbon et al., *Design and construction of the fast photon detection system for COMPASS RICH-1*, *Nucl. Instrum. Meth. A* **616** (2010) 21.

[4] P. Abbon et al., *Particle identification with COMPASS RICH-1*, *Nucl. Instrum. Meth. A* **631** (2011) 26.

[5] R. Chechik, A. Breskin, C. Shalem and D. Mormann, *Thick GEM-like hole multipliers: Properties and possible applications*, *Nucl. Instrum. Meth. A* **535** (2004) 303 [physics/0404119].

[6] Y. Giomataris, P. Rebourgeard, J.P. Robert and G. Charpak, *MICROMEGAS: A High granularity position sensitive gaseous detector for high particle flux environments*, *Nucl. Instrum. Meth. A* **376** (1996) 29.

[7] J. Agarwala et al., *The high voltage system with pressure and temperature corrections for the novel MPGD-based photon detectors of COMPASS RICH-1*, *Nucl. Instrum. Meth. A* **942** (2019) 162378.

[8] https://www.raspberrypi.org/products/raspberry-pi-3-model-b/.

[9] J. Agarwala et al., *The MPGD-Based Photon Detectors for the upgrade of COMPASS RICH-1 and beyond*, *Nucl. Instrum. Meth. A* **936** (2019) 416 [arXiv:1807.00816].

[10] S. Carrato et al., *A scalable High Voltage Power Supply System with system on chip control for Micro Pattern Gaseous Detectors*, *Nucl. Instrum. Meth.* **A** (2020) 163763.

[11] K.S. Mannatunga et al., *Design for portability of reconfigurable virtual instrumentation*, in *2019 X Southern Conference on Programmable Logic (SPL)*, Buenos Aires, Argentina (2019), p. 45–52 [DOI:10.1109/SPL.2019.8714446].

[12] F. Sauli, *Principle and operations of multiwire and drift chambers*, CERN-77-09 (1977).

[13] L.G.G. Ordóñez et al., *Multichannel Time Synchronization Based on PTP through a High Voltage Isolation Buffer Network Interface for Thick-GEM Detectors*, *Instruments* **6** (2022) 11.

2023 JINST 18 C07014